



Published in final edited form as:

Life Sci. 2020 September 15; 257: 118069. doi:10.1016/j.lfs.2020.118069.

Genetic disruption of the inflammasome adaptor ASC has minimal impact on the pathogenesis of Duchenne muscular dystrophy in *mdx* Mice

Yeh Siang Lau^{1,2}, Lixia Zhao¹, Chen Zhang¹, Haiwen Li¹, Renzhi Han^{1,*}

¹Department of Surgery, Davis Heart and Lung Research Institute, Biomedical Sciences Graduate Program, Biophysics Graduate Program, The Ohio State University Wexner Medical Center, Columbus, OH 43210, United States

²School of Healthcare and Medical Sciences, Sunway University, 47500, Bandar Sunway, Selangor, Malaysia

Abstract

Aim: Up-regulation of inflammasome proteins was reported in dystrophin-deficient muscles. However, it remains to be determined whether inflammasome activation plays a role in the pathogenesis of Duchenne muscular dystrophy. This study was therefore set out to investigate whether genetic disruption of the inflammasome pathway impacts the disease progression in *mdx* mice.

Main methods: Mice deficient in both dystrophin and ASC (encoded by *Pycard* [PYD And CARD Domain Containing]) were generated. The impact of ASC deficiency on muscular dystrophy of *mdx* mice were assessed by measurements of serum cytokines, Western blot, real-time PCR and histopathological staining.

Key findings: The pro-inflammatory cytokines such as TNF- α , IL-6, KC/GRO and IL-10 were markedly increased in the sera of 8-week-old *mdx* mice compared to WT. Western blotting showed that P2X7, caspase-1, ASC and IL-18 were upregulated. Disruption of ASC and dystrophin expression in the *mdx/ASC^{-/-}* mice was verified by Western blot analysis. Histopathological analysis did not find significant alterations in the muscular dystrophy phenotype in *mdx/ASC^{-/-}* mice as compared to *mdx* mice.

Significance: Taken together, our results show that disruption of the central adaptor ASC of the inflammasome is insufficient to alleviate muscular dystrophy phenotype in *mdx* mice.

* Address correspondence to: Renzhi Han, Ph.D., Department of Surgery, Davis Heart and Lung Research Institute, The Ohio State University Wexner Medical Center, Columbus, OH 43210, Phone: (614) 685-9214, renzhi.han@osumc.edu.

Publisher's Disclaimer: This is a PDF file of an unedited manuscript that has been accepted for publication. As a service to our customers we are providing this early version of the manuscript. The manuscript will undergo copyediting, typesetting, and review of the resulting proof before it is published in its final form. Please note that during the production process errors may be discovered which could affect the content, and all legal disclaimers that apply to the journal pertain.

Conflict of interest
None

Keywords

ASC; DMD; *mdx* mice; inflammasome; inflammation; muscle regeneration

1. Introduction

Duchenne muscular dystrophy (DMD) is an X-linked inherited neuromuscular disorder¹. It is the most common type of muscular dystrophy, caused by genetic mutations in *DMD*, the gene encoding dystrophin protein². Dystrophin is involved in forming a mechanical link between the cytoskeleton and the extracellular matrix, and thereby stabilizes the plasma membrane integrity through its interactions with other dystrophin-glycoprotein complex (DGC)^{3, 4}. The dystrophin protein is highly expressed in skeletal and cardiac muscles.

Studies of DMD prevalence suggest an average age at diagnosis in United States is from 5 to 9 years of age, affecting approximately 1 per 5,000 boys⁵. DMD has typically resulted in severe muscle wasting and loss of ambulation in their early teens, subsequently lead to respiratory and cardiac dysfunction and death between 20 and 40 years of age¹. Activation of innate inflammatory response has been well characterized in the pathology of muscular dystrophy due to the sarcolemmal instability after the disruption of DGC complex with the release of cytoplasmic contents and increased inflammatory immune cells infiltration including neutrophil and monocytes to the damage site and muscle tissue⁶⁻⁸. In severe muscle damage, the muscle tissue fails to repair where the regenerative capacity of myofibers is compromised. Excessive inflammation has been reported to be associated with the muscle tissue loss and fibrosis by increased production of proinflammatory cytokines⁹. Clinically, the overexpression of the proinflammatory cytokines such as tumor necrosis factor alpha (TNF- α), transforming growth factor beta (TGF- β), interleukin-1 (IL-1), and interleukin-6 (IL-6) has been reported in the muscle biopsies and serum samples from DMD patients, indicating that the inflammation may play an important role in pathogenesis of DMD¹⁰⁻¹³.

In recent years, increasing attention has been focused on the sterile inflammatory response that is activated by a large multimeric protein complex, known as inflammasome. Inflammasomes belong to the innate immune system and are composed of a sensor protein, an adaptor protein and a zymogen, procaspase-1. Several inflammasome complexes have been described including NLRP3 (nucleotide-binding domain leucine-rich repeat (NLR) and pyrin domain containing receptor 3), NLRP1, NLRC4, AIM2 (absent in melanoma 2). To date, the most described inflammasome is NLRP3 inflammasome, which consists of NLRP3, PYCARD (PYRIN-PAAD-DAPIN domain [PYD] and caspase recruitment domain [CARD] containing) adaptor, frequently referred to as apoptosis-associated speck-like protein (ASC), and pro-caspase-1^{14, 15}. Inflammasome is activated in the response to tissue damage or infection, which in turn activates procaspase-1 into active caspase-1. The active caspase-1 proteolytically activates cytokines interleukin-1 β (IL-1 β) and interleukin-18 (IL-18) and eventually induces an inflammatory form of cell death called pyroptosis¹⁵⁻¹⁷. Several studies have suggested a role of NLRP3 inflammasome in the pathogenesis of pulmonary hypertension, type 2 diabetes, liver damage, obesity-associated glomerular injury

and muscular dystrophy^{18–21}. Rawat *et al* (2010) has previously shown that the inflammasomes components and pro-inflammatory cytokine such as ASC, pro-caspase-1 and IL-1 β were upregulated in both dystrophin-deficient human (DMD) and *mdx* mouse skeletal muscle, indicating dystrophin-deficient induced activation of inflammasomes pathway. However, the contribution of the inflammasomes in the pathophysiology of DMD has not been well defined. This study aims to explore the effect of ASC deficiency on the pathology of muscular dystrophy.

2. Materials and methods

2.1 Mice.

All animal studies were reviewed and approved by the Institutional Animal Care and Use Committee (IACUC) of the Ohio State University. The *mdx* (C57BL/10ScSn-Dmd*mdx*/J) mice were purchased from the Jackson Laboratory (Bar Harbor, ME, USA). ASC deficient mice²² (a gift from Dr. Sutterwala) and *mdx* mice were intercrossed to generate mutant and control mice. Genotyping of ASC and *mdx* mice was performed by tail DNA PCR as previously described^{22, 23}. All mice were maintained at The Ohio State University Laboratory Animal Resources in accordance with animal use guidelines. All animal studies were authorized by the Animal Care, Use, and Review Committee of The Ohio State University.

2.2 Serum cytokine detection by ELISA.

The blood samples were collected from 8-week-old male WT, *mdx* and *mdx*/ASC^{-/-} mice before sacrificed. The blood was allowed to clot for 15 min to 30 min and centrifuged at 8000 rpm for 15 min in room temperature. The supernatant was collected as serum and stored at -80 °C for the cytokine detection assay. Cytokine levels were detected using MSD (Meso Scale Discovery, Rockville, MD) 10 panels V-PLEX mouse ELISA kit, following the manufacturer's protocol. The signal was collected with MESO QUICKPLEX SQ 120 and the data were analyzed using MSD Workbench 4.0 software.

2.3 Western blotting.

Quadriceps muscles were harvested from 8-week-old male WT, *mdx* and *mdx*/ASC^{-/-} mice. The tissues were homogenized with KINEMATICA Polytron™ PT 1300D Homogenizers (Bohemia, NY) and lysed with cold RIPA buffer (150 mM Sodium Chloride, 1% Triton X100, 0.5% sodium deoxycholate, 0.1% SDS, 50 mM Tris-HCl, 5 mM EDTA, pH 7.4) supplemented with protease inhibitors. The lysates were then centrifuged at 20,000 g for 20 min and supernatant was collected for Western blotting. The protein concentration of the supernatant was determined using the Lowry assay (Bio-Rad Laboratories, Hercules, CA, USA). Equal amount of extracted protein samples was separated by SDS-PAGE (BioRad, 4–20%) and transferred onto PVDF membranes (0.45 μ m). The blots were blocked for non-specific binding with 5% milk in Tris-buffered saline containing 0.1 % Tween 20 (TBS, pH 7.4) for 1 hour at room temperature with gentle shaking. After rinsing in TBS-T, the blots were incubated at 4°C overnight with primary antibodies against ASC (AL177, AG-25B-0006-C100, Adipogen International, San Diego, CA), caspase-1 (sc-514, Santa Cruz Biotechnology, Dallas, TX), P2X7 (ab109246, Abcam, Cambridge, MA), IL-18

(5180R; Biovision, Milpitas, California), IL-1 β (ab205924, Abcam) and dystrophin (E2660, Spring Bioscience, Pleasanton, CA). The blots were washed in TBS-T and incubated with respective secondary antibodies conjugated to horseradish peroxidase for 2 hours at room temperature. The blots were developed using ECL Western blotting substrate (Pierce Biotechnology, Rockford, IL) and images were captured using the ChemiDoc system (Bio-Rad Laboratories). The densitometric analysis was performed using Image Lab™ software, version 5.2.1 (Bio-Rad Laboratories). The respective protein expression levels were normalized to the housekeeping protein β -actin.

2.4 Immunofluorescence staining and histology.

Frozen muscle sections of 8 μ m were prepared from quadriceps of 8-week-old male WT, *mdx* and *mdx/ASC*^{-/-} mice. Immunofluorescence staining was performed as described previously²⁴. In brief, the slides were fixed with 4% paraformaldehyde for 15 minutes at room temperature and washed with PBS before blocked with 5% BSA for 1 hour. The slides were incubated with primary antibodies against eMyHC (F1.652, Developmental Studies Hybridoma Bank, University of Iowa, IA) and laminin α 2 (4H8/2, Alexis, San Diego, CA) at 4 °C overnight. After that, the slides were washed with PBS and incubated with secondary antibodies (Alexa Fluor 488 goat anti-rat IgG, Invitrogen, Carlsbad, CA or Alexa Fluor 594 goat anti-mouse IgG, Invitrogen) for 1h at room temperature. The slides were sealed with VECTASHIELD Antifade Mounting Medium with DAPI (vector laboratory, Burlingame, CA). Embryonic-MyHC-positive muscle fibers were counted and expressed as percentage of total number of positive fibers over total number of fibers in 10 fields. All images were taken under a Nikon Ti-E fluorescence microscope, magnification, X200 (Nikon, Melville, NY).

2.5 Histology.

For histological examinations, frozen muscle sections of 8 μ m were prepared from each group and were fixed in 4% paraformaldehyde for 15 minutes at room temperature. The slides were then proceeded to the standard protocol of hematoxylin and eosin (H&E), and Masson-trichrome staining to show myofiber morphology and assess collagen content. All images were taken under a Nikon Ti-E fluorescence microscope, magnification, X200 (Nikon, Melville, NY).

2.6 Serum Creatine Kinase Levels.

Creatine kinase (CK) levels were analyzed using the Creatine Kinase-SL assay kit (Sekisui Diagnostics, Lexington, MA) according to manufacturers' instructions. Briefly, 6 μ L of diluted serum sample was added accordingly to the 96-well UV microplate and following by 300 μ L of CK reagent. The plate was incubated at 30°C for 5 minutes and read in Flexstation 3 microplate reader (Molecular Devices, Sunnyvale, CA) for 2 min at 30 sec intervals.

2.7 Central nucleation counting

Frozen muscle sections were stained with anti-laminin α 2 antibody to delineate muscle fibers, and VECTASHIELD® Mounting Medium with DAPI was used for nuclear staining. All fibers, except those in direct contact with fascia, were analyzed for the location of their

nuclei. For each sample group, the number of fibers with centrally localized nuclei relative to the total number of fibers was recorded. For each individual mouse, about 2500–3500 fibers were counted.

2.8 Gene expression of IL-18 and IL-1 β .

Total RNA was extracted using RNeasy Mini Kit (Qiagen, USA) according to manufacturer's instruction. Then 5 μ g RNA was reverse transcribed using RevertAid RT Reverse Transcription Kit (Thermo Scientific, USA). Quantitative PCR was carried out using the Radiant™ SYBR Green qPCR kits (Alkali Scientific, Pompano Beach, FL). The IL-18 forward and reverse primer sequences were 5'-AAAGTGCCAGTGAACCC-3' and 5'-TTTGATGTAAGTTAGTGAGAGTGA-3' respectively. The IL-1 β forward and reverse primer sequences were 5'-CACAGCAGCACATCAACAAG-3' and 5'-GTGCTCATGTCCTCATCCTG-3' respectively. Each assay was run on a LightCycler® 480 System (Roche Diagnostics Corporation, IN, USA) in triplicate and the results are calculated using the relative standard curve method. All gene expressions were normalized against the respective housekeeping gene GAPDH.

2.9 Statistics.

The data were expressed as mean \pm SEM and analyzed with GraphPad Prism 5.0 software (San Diego, USA). Statistical significance was determined using one-way ANOVA followed by Bonferroni post hoc-tests or unpaired 2-tailed Student's t test whenever appropriate. A P value of less than 0.05 is regarded as significant.

3. Results

3.1 Serum inflammatory cytokine profile in mdx mice

When cells die by necrosis they stimulate a robust acute inflammatory response *in vivo*²⁵. Repeated muscle injury in the absence of dystrophin occurs, which persistently activates the immune system and causes muscle inflammation. We first examined the inflammatory profile in *mdx* mice by measuring inflammatory cytokines in the serum samples of 8-week-old *mdx* mice. The pro-inflammatory cytokines such as TNF- α , IL-6, KC/GRO and IL-10 were significantly increased in *mdx* mice compared to WT (Figure 1). The serum levels of IL-1 β appeared to be increased in *mdx* mice, although the difference did not reach statistical significance.

3.2 Up-regulation of inflammasome proteins in mdx muscles

A number of cellular contents such as uric acid, HMGB1, SAP130, IL-1 α , IL-33, DNA, S100 proteins, heat shock proteins and others, are released upon necrotic cell injury, which are believed to contribute to death-induced inflammation. The NLRP3 inflammasome, part of innate immune system, has been known to participate in the sterile inflammatory response, which may further exacerbate muscle pathology in muscular dystrophy. Next, our Western blotting results demonstrated a significant increase of P2X7 receptor, an ATP-gated ion channel in *mdx* mice relative to WT control. As expected, the biomarkers for activation of inflammasomes protein complex were found upregulated including caspase-1, ASC and

IL-18, in muscle lysates from *mdx* mice (Figure 2). Our data also confirmed the signature protein expression of dystrophin was absent in *mdx* mice (Figure 2A).

3.3 Effect of ASC deficiency on muscle pathology in *mdx* mice

To study if blockade of the NLRP3 inflammasome ameliorates muscular dystrophy pathology, we generated a double knockout (DKO) mouse strain with deficiency in both dystrophin and ASC, an inflammasome adaptor protein. The mice genotyped by tail DNA PCR were verified by Western blot analysis. Disruption of dystrophin and ASC expression was confirmed in the muscle lysates of the *mdx*/ASC DKO mice (Figure 3).

Repeated muscle degeneration and regeneration is a histopathological hallmark of muscular dystrophy, as indicated by the presence of muscle necrosis and central nucleated muscle fibers (CNF). The *quadriceps* and *gastrocnemius* muscles were assessed in H&E staining. As shown in the top panel of Figure 4A, both the *mdx* and *mdx*/ASC DKO muscles exhibited various size of muscle fibers, presence of internal nuclei, and increased fibrotic area. To quantify some of the pathological features, we stained the muscle sections with laminin $\alpha 2$ (to demarcate the muscle fibers) and 4',6-diamidino-2-phenylindole (DAPI, to label nuclei) (Figure 4A, bottom). Both *mdx* and *mdx*/ASC DKO muscles had significantly increased CNFs as compared to WT controls, but there was no significant difference between *mdx* and *mdx*/ASC DKO muscles (Figure 4B). Due to the presence of smaller, regenerating muscle fibers in dystrophic muscles, the average cross-sectional area (CSA) of muscle fibers were significantly decreased in both *mdx* and *mdx*/ASC DKO muscles (Figure 4C). Again, we observed no difference in CSA between *mdx* and *mdx*/ASC DKO muscles (Figure 4C). Moreover, the fiber size distribution was similarly altered in *mdx* and *mdx*/ASC DKO muscles as compared to WT controls (Figure 4D). Consistently, we observed that the serum creatine kinase (CK) levels were similarly increased in both *mdx* and *mdx*/ASC DKO mice (Figure 4E).

To further investigate if ASC disruption has any impact on muscle regeneration in *mdx* mice, embryonic myosin heavy chain (eMyHC), a marker of newly regenerated muscle fibers, was assessed. Both *mdx* and *mdx*/ASC DKO muscles exhibited increased number of eMyHC-positive fibers compared to WT (Figure 5A & B). However, no statistically significant changes were observed between *mdx*/ASC DKO and *mdx*.

4. Discussion

In this study, we found that the inflammasome proteins were up-regulated in the skeletal muscle of *mdx* mice, which also displayed an altered inflammation cytokine profile in the serum. However, genetic disruption of the inflammasome adaptor ASC in the *mdx* mice did not significantly improve the muscle pathology. Our results cast doubt on the feasibility of targeting inflammasome as a therapeutic strategy for DMD.

During sterile tissue damage, the immune system, particularly the inflammasome, has been implicated in many pathological conditions including DMD. Rawat *et al.* (2010) showed an increased expression of ASC and caspase-1²⁰ in muscle biopsies of DMD patients. In consistent with these previous observations, we also found that the expression of P2X7,

ASC, caspase-1 and IL-1 β were significantly increased. These findings suggest a potential role of inflammasome activation in the pathogenesis of muscular dystrophy. Indeed, a previous study showed that genetic ablation of NLRP3 appeared to reduce the muscle pathology, inflammation and oxidative stress in *mdx* mice²⁶. Ghrelin, a circulating hormone was found to suppress muscle inflammation and ameliorate disease phenotype in *mdx* mice via inhibition of NLRP3 inflammasome²⁷. In addition, several other studies have shown that pharmacological blockade of P2X7 receptors reduced muscle inflammation and improve muscle pathology in *mdx* mice^{28–30}.

Given the promising previous observations mentioned above, it is surprising that genetic disruption of the inflammasome adaptor protein ASC had little impact on the muscle pathology in dystrophic mice as shown by our present study. As a central player of the NLRP3 inflammasome, ASC is a bipartite molecule that contains both an N-terminal PYD and a C-terminal CARD, allowing it to bridge the sensor NLRP3 and the effector pro-caspase-1³². The deletion or silencing of ASC has been reported to reduce hypoxia-induced pulmonary hypertension and high fat diet-induced podocyte injury^{18, 21}. It is unclear what exactly underlies the discrepancy between our study and others, however, numerous studies have shown that NLRP3 may act via an inflammasome-independent mechanism, which may or may not require ASC. For example, hypoxia induced significant increase of NLRP3, independent of ASC, caspase-1 and IL-1 β , which mediated mitochondrial regulation in renal injury³¹. NLRP3-deficient and ASC-deficient mice show difference in survival and early renal dysfunction following renal ischemic injury³². NLRP3 deficiency or inhibition via β -hydroxybutyrate precursor 1,3-butanediol protected the mice from nephrocalcinosis-related chronic kidney disease (CKD), but IL-1 inhibitor had no such protective effect, suggesting that NLRP3 has an IL-1-independent function in CKD³³. During the NLRP3-mediated Epithelial-Mesenchymal Transition process induced by TNF- α or TGF- β 1, the cleaved caspase-1 and ASC speck were not detected in mesenchymal-like colon cancer cells, indicating that NLRP3 functions in an inflammasome-independent way³⁴. Moreover, NLRP3 was found to be required for resistance to pneumococcal pneumonia, whereas caspase-1 and caspase-11 were dispensable in *S. pneumoniae*-infected mice³⁵. Thus, it is possible that the ASC-independent role of NLRP3 is involved in muscle pathology of *mdx* mice. Even more complicated, the sterile inflammatory responses are often only partially reduced and in some cases seem largely independent of the inflammasome components as demonstrated by the use of NLRP3-deficient animals³⁶. Other cellular processes such as autophagy may also be involved in tissue inflammation³⁷. Therefore it is possible that the mechanisms operating *in vivo* are more complicated and may involve redundant pathways. Disruption of one aspect of the immune system may be well compensated by the presence of the other redundant pathways.

5. Conclusions

This study shows that ASC knockout has minimal impact on muscle pathology of *mdx* mice. This finding suggests that targeting ASC may not be sufficient for alleviating muscle pathology in DMD. Further investigations are needed to better understand the inflammasome-dependent and independent functions of ASC and NLRP3 in muscular dystrophy.

Acknowledgements

This work was supported by US National Institutes of Health grants R01-HL116546 and R01-AR064241 to R.H.

References

1. D'Amario D et al. A current approach to heart failure in Duchenne muscular dystrophy. *Heart* (2017).
2. Nowak KJ & Davies KE Duchenne muscular dystrophy and dystrophin: pathogenesis and opportunities for treatment. *EMBO reports* 5, 872–876 (2004). [PubMed: 15470384]
3. Gao QQ & McNally EM The Dystrophin Complex: Structure, Function, and Implications for Therapy. *Comprehensive Physiology* 5, 1223–1239 (2015). [PubMed: 26140716]
4. Allen DG, Whitehead NP & Froehner SC Absence of Dystrophin Disrupts Skeletal Muscle Signaling: Roles of Ca²⁺, Reactive Oxygen Species, and Nitric Oxide in the Development of Muscular Dystrophy. *Physiological reviews* 96, 253–305 (2016). [PubMed: 26676145]
5. Romitti PA et al. Prevalence of Duchenne and Becker muscular dystrophies in the United States. *Pediatrics* 135, 513–521 (2015). [PubMed: 25687144]
6. Falzarano MS, Scotton C, Passarelli C & Ferlini A Duchenne Muscular Dystrophy: From Diagnosis to Therapy. *Molecules* 20, 18168–18184 (2015). [PubMed: 26457695]
7. Tidball JG & Villalta SA Regulatory interactions between muscle and the immune system during muscle regeneration. *American journal of physiology. Regulatory, integrative and comparative physiology* 298, R1173–1187 (2010).
8. Rosenberg AS et al. Immune-mediated pathology in Duchenne muscular dystrophy. *Science translational medicine* 7, 299rv294 (2015).
9. Costamagna D, Costelli P, Sampaolesi M & Penna F Role of Inflammation in Muscle Homeostasis and Myogenesis. *Mediators of inflammation* 2015, 805172 (2015). [PubMed: 26508819]
10. De Paepe B & De Bleecker JL Cytokines and chemokines as regulators of skeletal muscle inflammation: presenting the case of Duchenne muscular dystrophy. *Mediators of inflammation* 2013, 540370 (2013). [PubMed: 24302815]
11. Saito K et al. A sensitive assay of tumor necrosis factor alpha in sera from Duchenne muscular dystrophy patients. *Clinical chemistry* 46, 1703–1704 (2000). [PubMed: 11017956]
12. Wright CR et al. A Reduction in Selenoprotein S Amplifies the Inflammatory Profile of Fast-Twitch Skeletal Muscle in the mdx Dystrophic Mouse. *Mediators of inflammation* 2017, 7043429 (2017). [PubMed: 28592916]
13. Cruz-Guzman Odel R, Rodriguez-Cruz M & Escobar Cedillo RE Systemic Inflammation in Duchenne Muscular Dystrophy: Association with Muscle Function and Nutritional Status. *BioMed research international* 2015, 891972 (2015). [PubMed: 26380303]
14. He Y, Hara H & Nunez G Mechanism and Regulation of NLRP3 Inflammasome Activation. *Trends in biochemical sciences* 41, 1012–1021 (2016). [PubMed: 27669650]
15. Vanaja SK, Rathinam VA & Fitzgerald KA Mechanisms of inflammasome activation: recent advances and novel insights. *Trends in cell biology* 25, 308–315 (2015). [PubMed: 25639489]
16. Latz E, Xiao TS & Stutz A Activation and regulation of the inflammasomes. *Nature reviews. Immunology* 13, 397–411 (2013).
17. Guo H, Callaway JB & Ting JP Inflammasomes: mechanism of action, role in disease, and therapeutics. *Nature medicine* 21, 677–687 (2015).
18. Cero FT et al. Absence of the inflammasome adaptor ASC reduces hypoxia-induced pulmonary hypertension in mice. *American journal of physiology. Lung cellular and molecular physiology* 309, L378–387 (2015). [PubMed: 26071556]
19. Masters SL et al. Activation of the NLRP3 inflammasome by islet amyloid polypeptide provides a mechanism for enhanced IL-1beta in type 2 diabetes. *Nature immunology* 11, 897–904 (2010). [PubMed: 20835230]
20. Rawat R et al. Inflammasome up-regulation and activation in dysferlin-deficient skeletal muscle. *The American journal of pathology* 176, 2891–2900 (2010). [PubMed: 20413686]

21. Boini KM et al. Activation of inflammasomes in podocyte injury of mice on the high fat diet: Effects of ASC gene deletion and silencing. *Biochimica et biophysica acta* 1843, 836–845 (2014). [PubMed: 24508291]
22. Sutterwala FS et al. Critical role for NALP3/CIAS1/Cryopyrin in innate and adaptive immunity through its regulation of caspase-1. *Immunity* 24, 317–327 (2006). [PubMed: 16546100]
23. Shin JH, Hakim CH, Zhang K & Duan D Genotyping mdx, mdx3cv, and mdx4cv mice by primer competition polymerase chain reaction. *Muscle Nerve* 43, 283–286 (2011). [PubMed: 21254096]
24. Xu L et al. CRISPR-mediated Genome Editing Restores Dystrophin Expression and Function in mdx Mice. *Molecular therapy : the journal of the American Society of Gene Therapy* 24, 564–569 (2016). [PubMed: 26449883]
25. Chen CJ et al. Identification of a key pathway required for the sterile inflammatory response triggered by dying cells. *Nature medicine* 13, 851–856 (2007).
26. Boursereau R, Abou-Samra M, Lecompte S, Noel L & Brichard SM Downregulation of the NLRP3 inflammasome by adiponectin rescues Duchenne muscular dystrophy. *BMC Biol* 16, 33 (2018). [PubMed: 29558930]
27. Chang L et al. Ghrelin improves muscle function in dystrophin-deficient mdx mice by inhibiting NLRP3 inflammasome activation. *Life Sci* 232, 116654 (2019). [PubMed: 31306657]
28. Al-Khalidi R et al. Zidovudine ameliorates pathology in the mouse model of Duchenne muscular dystrophy via P2RX7 purinoceptor antagonism. *Acta Neuropathol Commun* 6, 27 (2018). [PubMed: 29642926]
29. Gazzero E et al. Enhancement of Muscle T Regulatory Cells and Improvement of Muscular Dystrophic Process in mdx Mice by Blockade of Extracellular ATP/P2X Axis. *Am J Pathol* 185, 3349–3360 (2015). [PubMed: 26465071]
30. Sinadinos A et al. P2RX7 purinoceptor: a therapeutic target for ameliorating the symptoms of duchenne muscular dystrophy. *PLoS Med* 12, e1001888 (2015). [PubMed: 26461208]
31. Kim SM et al. Inflammasome-Independent Role of NLRP3 Mediates Mitochondrial Regulation in Renal Injury. *Front Immunol* 9, 2563 (2018). [PubMed: 30483252]
32. Iyer SS et al. Necrotic cells trigger a sterile inflammatory response through the Nlrp3 inflammasome. *P Natl Acad Sci USA* 106, 20388–20393 (2009).
33. Anders HJ et al. The macrophage phenotype and inflammasome component NLRP3 contributes to nephrocalcinosis-related chronic kidney disease independent from IL-1-mediated tissue injury. *Kidney Int* 93, 656–669 (2018). [PubMed: 29241624]
34. Wang H et al. Inflammasome-independent NLRP3 is required for epithelial-mesenchymal transition in colon cancer cells. *Exp Cell Res* 342, 184–192 (2016). [PubMed: 26968633]
35. Fang RD et al. ASC and NLRP3 maintain innate immune homeostasis in the airway through an inflammasome-independent mechanism. *Mucosal Immunol* 12, 1092–1103 (2019). [PubMed: 31278375]
36. Rock KL, Latz E, Ontiveros F & Kono H The sterile inflammatory response. *Annual review of immunology* 28, 321–342 (2010).
37. Saitoh T et al. Loss of the autophagy protein Atg16L1 enhances endotoxin-induced IL-1beta production. *Nature* 456, 264–268 (2008). [PubMed: 18849965]

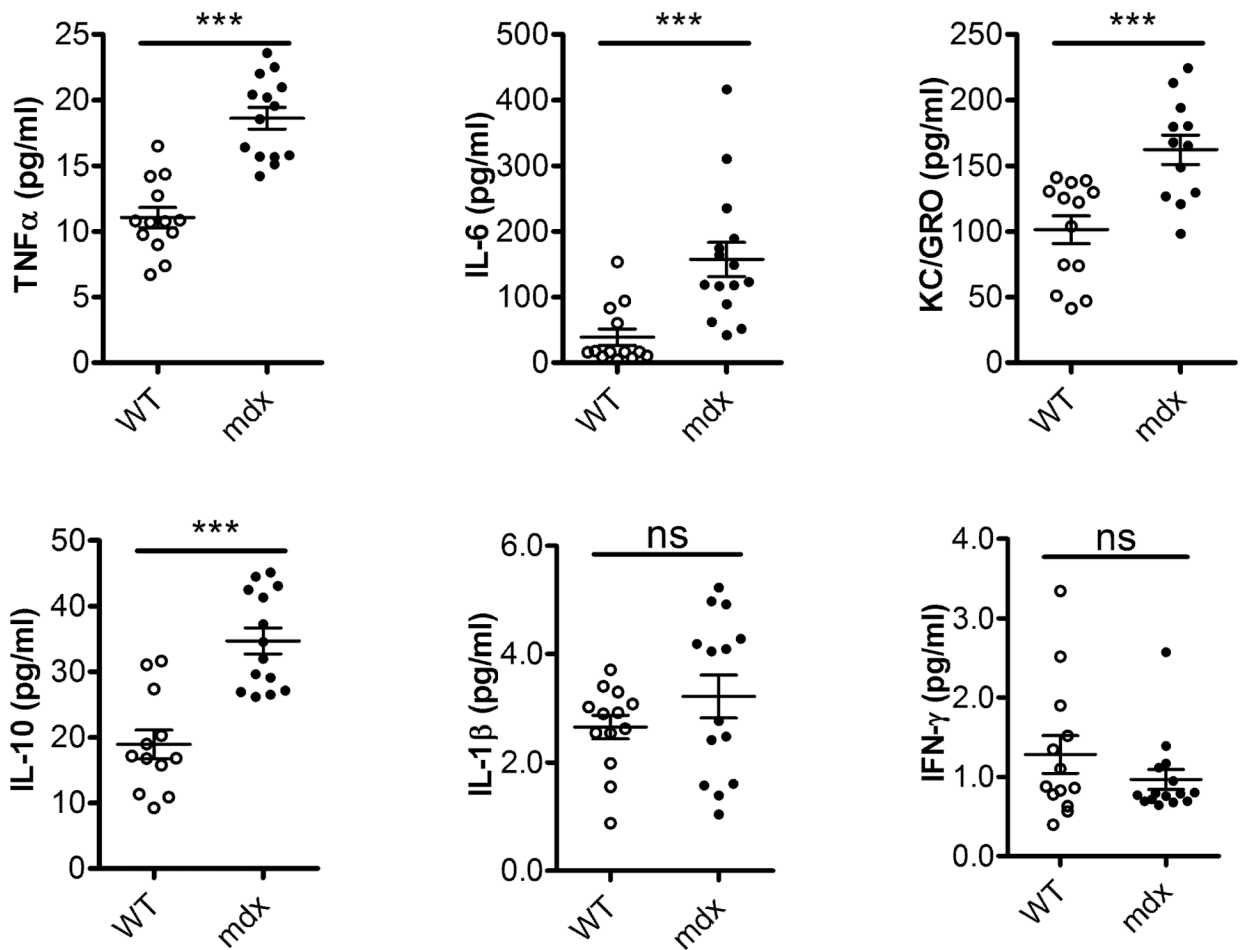


Figure 1.

Upregulation of pro-inflammatory cytokines in *mdx* mice. The serum cytokines profile was measured by ELISA in WT and *mdx* mice. The pro-inflammatory cytokines, TNF- α , IL-6, KC/GRO and IL-10 were increased in 8-week-old *mdx* mice compared to WT. Results are shown as mean \pm SEM, n = 12–14, ***P < 0.001 compared with WT.

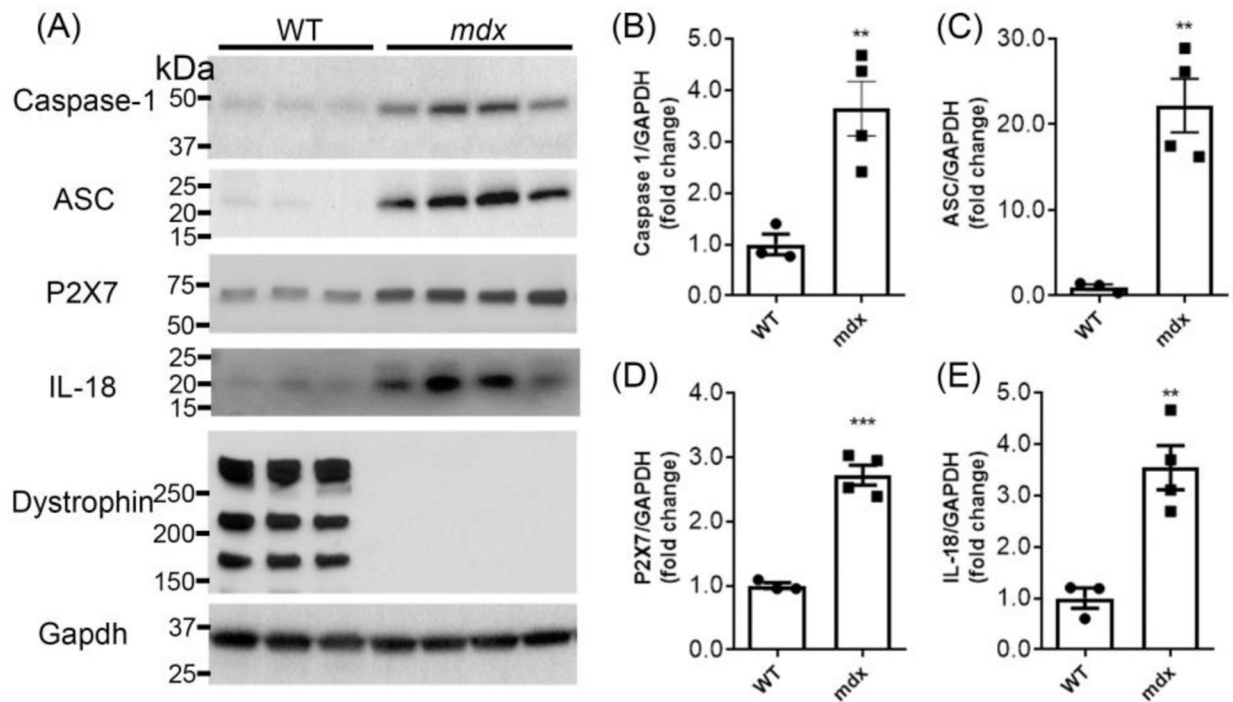


Figure 2.

Inflammasome signaling proteins upregulated in *mdx* mice. (A) The Western blotting shows upregulation of P2X7, caspase-1, ASC and IL-18 and absence of dystrophin protein in muscle lysates from *mdx* mice. (B-E) Graphs show quantitation analysis of Western blots.

** $P < 0.01$, *** $P < 0.001$ compared with WT.

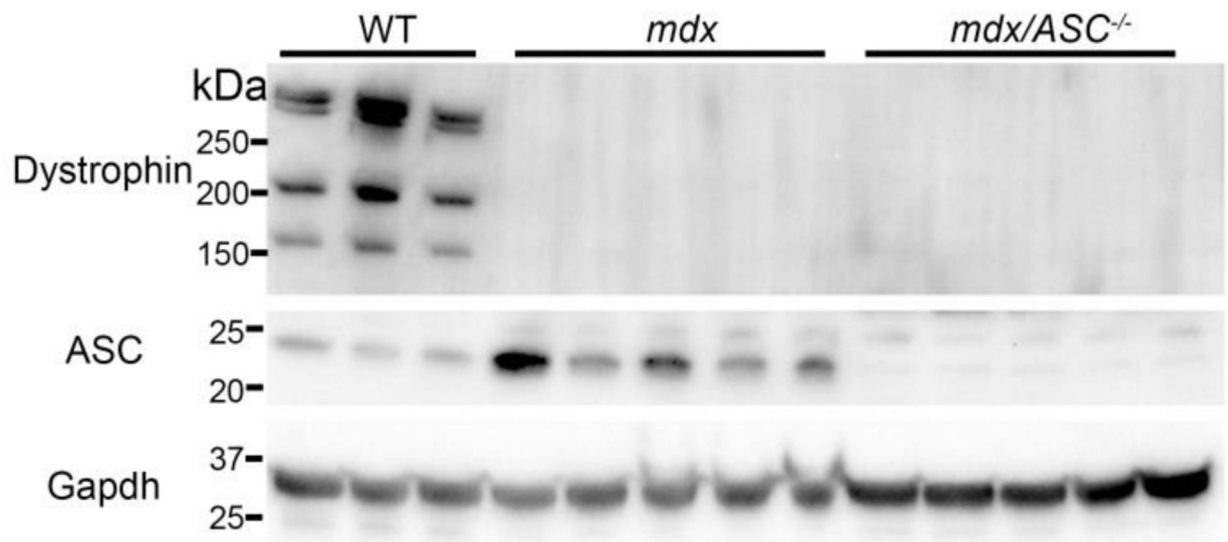


Figure 3. Western blot analysis of muscle lysates from WT, *mdx* and *mdx/ASC* DKO mice. Western blotting shows upregulation of ASC and absence of dystrophin protein in muscle lysates from *mdx* mice and absence of both dystrophin and ASC protein in *mdx/ASC* DKO mice.

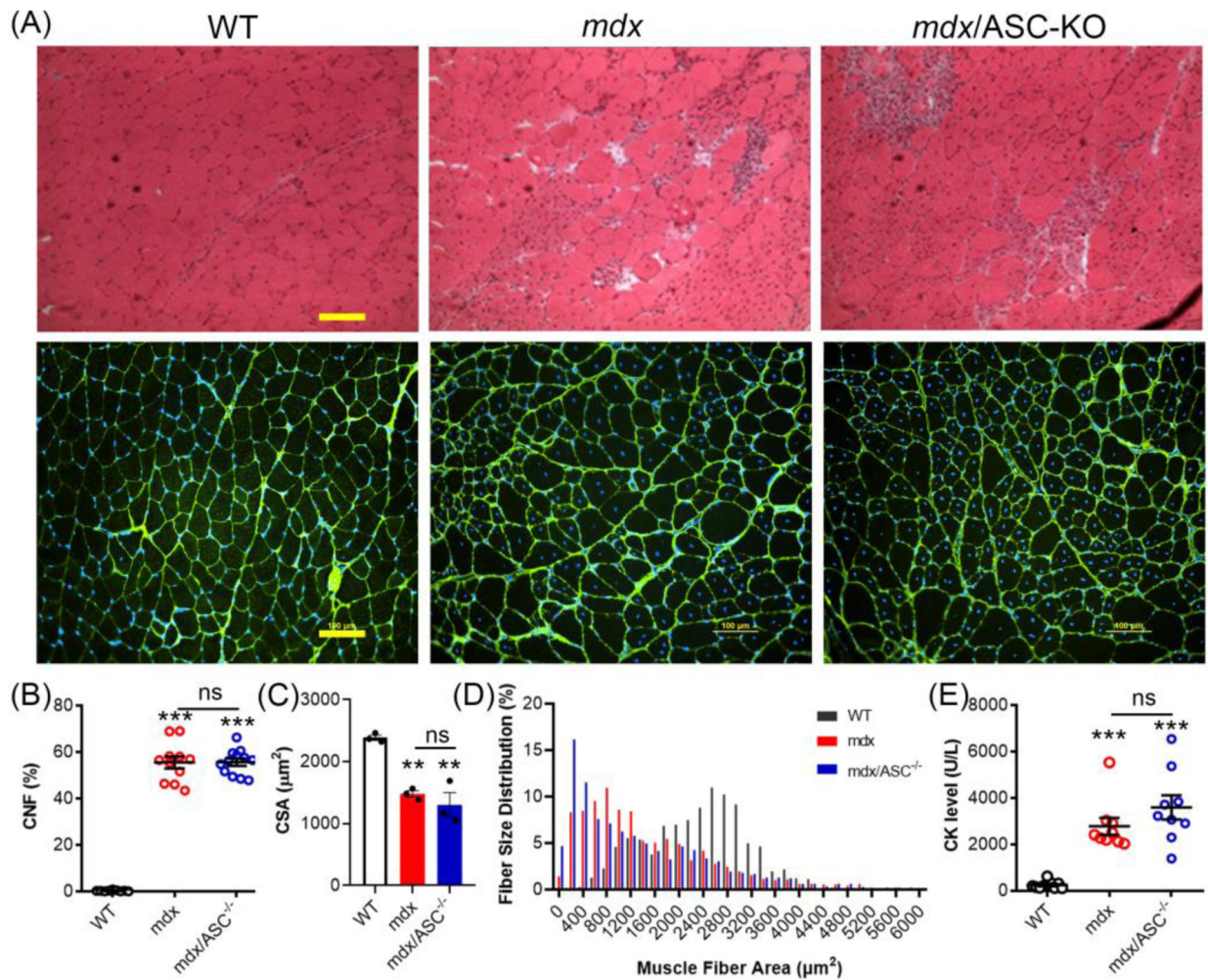


Figure 4.

ASC disruption had minimal impact on the dystrophic pathology of *mdx* mice. (A) H&E (top panel) and laminin α 2/DAPI (bottom panel) stained histological sections of quadriceps from WT, *mdx* and *mdx/ASC^{-/-}* mice. (B) Percentage of central nucleated fibers (CNF) in muscle sections of WT, *mdx* and *mdx/ASC^{-/-}* mice. (C) Average cross-sectional area (CSA) of muscle fibers in WT, *mdx* and *mdx/ASC^{-/-}* mice. (D) Muscle fiber size distribution of WT, *mdx* and *mdx/ASC^{-/-}* mice. (E) Serum creatine kinase (CK) levels of WT, *mdx* and *mdx/ASC^{-/-}* mice. *** $P < 0.001$ compared with WT; ns, not statistically significant.

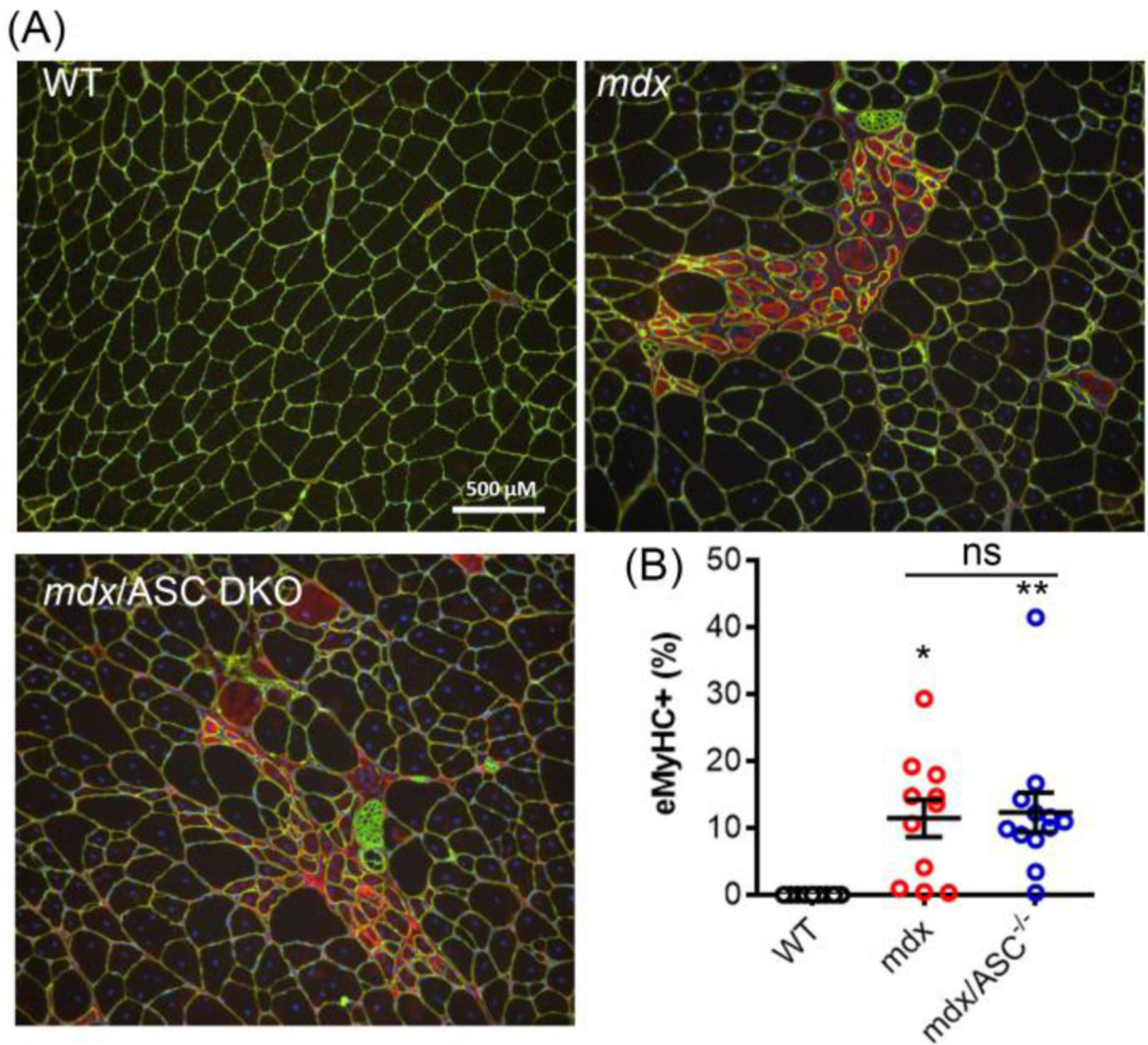


Figure 5. Muscle regeneration was similar in *mdx* and *mdx/ASC DKO* mice. Representative immunofluorescence images (A) and quantitation (B) of eMyHC (red) from quadriceps of different mouse groups. Muscle fibers were co-stained with laminin 2 α (green). * $P < 0.05$, ** $P < 0.01$, compared with WT; ns, not statistically significant.